Ordered phase of the O(N) model within the nonperturbative renormalization group

Marcela Peláez and Nicolás Wschebor
Instituto de Física, Facultad de Ingeniería, Universidad de la República, J.H.y Reissig 565, 11000 Montevideo, Uruguay
(Received 22 October 2015; revised manuscript received 26 July 2016; published 26 October 2016)

We analyze nonperturbative renormalization group flow equations for the ordered phase of $\mathbb{Z}_2$ and O(N) invariant scalar models. This is done within the well-known derivative expansion scheme. For its leading order [local potential approximation (LPA)], we show that not every regulator yields a smooth flow with a convex free energy and discuss for which regulators the flow becomes singular. Then we generalize the known exact solutions of smooth flows in the "internal" region of the potential and exploit these solutions to implement an improved numerical algorithm, which is much more stable than previous ones for $N > 1$. After that, we study the flow equations at second order of the derivative expansion and analyze how and when the LPA results change. We also discuss the evolution of the field renormalization factors.

DOI: 10.1103/PhysRevE.94.042136

I. INTRODUCTION

The low temperature properties of most equilibrium statistical systems draw great physical interest. For example, they include the liquid phase in the liquid-vapor transition or the ferromagnetic phase of a magnet. Among the quantities of interest on these phases is the effective potential that determines the equation of state (and, for example, the magnetization as a function of the temperature in a magnet). These properties are often disregarded for many reasons. First, they are nonuniversal (they depend on the microscopic Hamiltonian of the system). Second, they are difficult to handle because typically the low temperature phase includes intense interactions that are very difficult to treat within standard perturbative means. More precisely, the low temperature regime of typical statistical models is notoriously more difficult to handle than the high temperature one. At low temperature, it is usual that the coexistence of two different phases dominates the free energy and this property is not easily handled by mean field methods or perturbative expansions. This manifests itself as violations of various exact thermodynamics properties at mean field level, such as the convexity of the free energy in terms of the order parameter. Convexity can be restored by hand in mean field treatments via the Maxwell construction but it is unclear how this strategy can be followed systematically when a perturbative expansion is performed around the mean field. The reason is that convexity in the coexistence region is associated with large fluctuations in the configuration space and not with small ones around a mean field analysis. Another difficulty is that such large distance effects must be analyzed together with short distance behavior that typically dominates nonuniversal properties as the phase diagram. One then needs a method capable of treating all phenomena including very different length scales.

Since the 1990s a method has been developed [the so-called nonperturbative renormalization group [1–5] (NPRG)], that can easily handle the convexity properties of the free energy. It was quickly understood [6–12] that one of the simplest approximations implemented in such a scheme naturally yields a convex free energy. This approximation scheme, called local potential approximation (LPA), is also able to address successfully a large variety of statistical problems at equilibrium, out of equilibrium (for reviews on the subject see for example [13–15]), or even in more difficult contexts, such as in the presence of quenched disorder (see for example [16]). Moreover, this approximation scheme can be seen as the leading order of a systematic expansion of vertex functions in wave numbers called the derivative expansion (DE) [13,14,17]. The DE has shown to be extremely successful [13,14]. It has been pushed in the case of a single scalar Ginzburg-Landau model up to order $O(\partial^4)$ [18] obtaining results with a quality comparable to those of Borel resummed six order perturbative expansion.[1]

Given these previous results it is natural to extend the analysis to higher orders of the DE for models with O(N) symmetry [12]. One of the difficulties is that although the LPA preserves the convexity of the free energy, its numerical implementation is generically unstable: at sufficiently small RG scales, the numerical flow becomes unstable. Even if the convexity shows up, the free energy approaches singular points of the flow equations and it is difficult to push the solution numerically to low momentum scales. This is in radical contrast with what happens in the high temperature phase or around a critical point. Given this problem, sophisticated numerical methods have been employed in order to solve the LPA equation at low renormalization group scales [11,20,21]. The difficulty with such approaches is that they are difficult to implement at next-to-leading orders of DE and even more difficult when applied to more sophisticated approximation schemes such as the Blaizot-Méndez-Wschebor scheme [22–24].

A word can be said on the comparison of NPRG results within the DE with Monte Carlo simulations. One could wonder what is the point of using semianalytical results if one has at our disposal simulations that can, at least in principle for most models, be made as precise as we want. While simulations are extremely useful, NPRG analysis can be a valuable complement for many reasons. First, even if NPRG approximations are usually harder to control than systematics in Monte Carlo simulations, some of the systematics of simulations are not present in NPRG. For example, NPRG studies can cover orders of magnitudes in length scales and they are not limited by finite volumes or coarse lattices.

[1]The analysis of the derivative expansion at order $O(\partial^6)$ [19] has been presented in various conferences.

 ©2016 American Physical Society

Moreover, the numerical cost of NPRG studies is usually many orders of magnitude lower than Monte Carlo studies. In practice, it is convenient to exploit in a complementary way both approaches.

One last comment is necessary before going to the content of the article. One could consider two ways to avoid the analysis of the approach of the convexity of free energy. In fact, one must frequently consider the free energy in an external magnetic field (or, for liquid-vapor transition in the presence of a chemical potential). At a uniform nonzero external field, in many cases the behavior of the free energy stabilizes before the singularities associated with the approach to the convexity take place. In such a case, one could just stop the flow and ignore the regions of the free energy with a nonconvex behavior. The problem with such an approach is that the systematic errors associated with such procedures can not be made arbitrary small. Moreover, in many cases the singularities are approached *before* the nonflat part of the free energy stabilizes. This does not exclude the use of this procedure but limits its range of applicability. For example, this procedure, together with the approximation proposed in [22], has been exploited recently with success in the study of bound states in 3-d scalar theories in the ordered phase near the critical point [25] but it is unclear whether such procedure can be used at lower temperatures. The second strategy is to consider the possibility of making a field expansion around the minimum of the potential [13]. This, in a way, decouples the physics of the "nonconvex" part of the potential from the convex one. However, the field expansion works very badly at dimensions lower than three even at criticality (it breaks down even at very high order of the expansion at dimensions around 2.8 because of the proliferation of multicritical points [26]). Even in dimension three and higher, this procedure is unable to treat the case of first order phase transitions or cases where the full field behavior is needed. This is important in order to have access to the equation of state or even to study the phase diagram, for example, in the liquid-vapor transition where no symmetry $\mathbb{Z}_2$ is present far from the critical point.

In the present article, we extend previous studies of the low temperature phase of Ginzburg-Landau models within the NPRG. First, we improve previous results in the LPA approximation to the O(N) model, analyzing in detail the dependence in the regulator and the number of fields. We show that, contrarily to what could be expected, the numerical behavior of flow equations is much more stable when $N > 1$ than for $N = 1$. In both cases we improve and exploit analytical results for the free energy in the coexistence region in order to implement a simple numerical algorithm that allows us to explore much smaller renormalization group momentum scales. Then, we extend the numerical results for O(N) models to the DE at next-to-leading order.

II. NONPERTURBATIVE RENORMALIZATION GROUP AND THE DERIVATIVE EXPANSION

Before considering the behavior of the effective action in the low temperature phase, let us recall briefly the origin and uses of NPRG equations. We present this formalism for a generic Euclidean field theory with N scalar fields φ_i, denoted collectively by φ, with Hamiltonian $H[\varphi]$. Then, we specialize to the case where $H[\varphi]$ is O(N) or $\mathbb{Z}_2$ symmetric. The NPRG equations, intimately related to Wilsonian renormalization group equations, connect the Hamiltonian to the full Gibbs free energy (generating functional of 1-PI vertex functions). This relation is obtained by controlling the magnitude of long wavelength field fluctuations with the help of an infrared cutoff, which is implemented [3–5,27] by adding to the Hamiltonian $H[\varphi]$ a regulator of the form

$$\Delta H_k[\varphi] = \frac{1}{2}\int \frac{d^d q}{(2\pi)^d}[R_k(q)]_{ij}\varphi_i(q)\varphi_j(-q), \qquad (1)$$

where $[R_k(q)]_{ij}$ denotes a family of k-dependent "cutoff functions" to be specified below. Above and below, sums are understood for repeated internal indices. The role of ΔH_k is to suppress the fluctuations of $\varphi(q)$ with momenta $q \lesssim k$, while leaving unaffected the modes with $q \gg k$. Accordingly, typically $R_k(q)_{ij} \sim k^2\delta_{ij}$ when $q \ll k$, and $R_k(q)_{ij} \to 0$ quickly when $q \gtrsim k$. Therefore, the partition function with an external source J is modified as

$$Z_k[J] = \int \mathcal{D}\varphi \, \exp\left\{-H[\varphi] - \Delta H_k[\varphi] + \int J\varphi\right\}. \qquad (2)$$

One can define an effective Gibbs free energy corresponding to $H[\varphi] + \Delta H_k[\varphi]$ denoted by $\Gamma_k[\phi]$ as a (modified) Legendre transformation of the free energy given by

$$\Gamma_k[\phi] = -\ln Z_k[J] + \int J\varphi - \Delta H_k[\phi], \qquad (3)$$

where ϕ is the average field; $\phi_i(x) = \langle\varphi_i(x)\rangle$ in the presence of external sources. When $k = \Lambda$, with Λ the microscopic scale of the problem, all fluctuations are suppressed and $\Gamma_\Lambda[\phi]$ coincides with the Hamiltonian. As k is lowered, more and more fluctuations are taken into account and when $k \to 0$, all fluctuations are included and $\Gamma_{k=0}[\phi]$ becomes the Gibbs free energy $\Gamma[\phi]$ (see, e.g., [13]). The flow of $\Gamma_k[\phi]$ with k is given by the Wetterich equation [3–5,27]:

$$\partial_k\Gamma_k[\phi] = \frac{1}{2}\int \frac{d^d q}{(2\pi)^d}\mathrm{tr}\left\{\partial_k R_k(q^2)\left[\Gamma_k^{(2)} + R_k\right]^{-1}_{q;-q}\right\}, \qquad (4)$$

where $\Gamma_k^{(2)}$ denotes the matrix of second derivatives of Γ_k with respect to ϕ and the trace is taken over internal indices.

From now on, we specialize to O(N)-symmetric models. Since we are interested in the following in nonuniversal properties such as the free-energy for $T < T_c$, we need in principle to consider general O(N)-invariant Hamiltonians. NPRG equations have no difficulties in handling non-renormalizable Hamiltonians and can even include a realistic microscopic structure of a given system such as a specific lattice model in order to analyze nonuniversal properties [28,29]. However, for the purposes of the present article it is enough to choose a simple φ^4 Ginzburg-Landau Hamiltonian given by

$$H[\varphi] = \int d^d x \left\{\frac{1}{2}\nabla\varphi_i(x)\cdot\nabla\varphi_i(x) + \frac{r}{2}\varphi_i(x)\varphi_i(x) + \frac{u}{4!}[\varphi_i(x)\varphi_i(x)]^2\right\}. \qquad (5)$$

In order to preserve the O(N) symmetry all along the flow, it is mandatory to consider a regulator respecting this symmetry.

This implies the use of a regulator of the form

$$[R_k(q)]_{ij} \equiv R_k(q)\delta_{ij}.$$

In practice, we choose functions $R_k(q)$ of the two types most frequently used in the literature. The first one corresponds to the θ regulator [30] equal, up to field renormalizations, to

$$R_k(q) = (k^2 - q^2)\theta(1 - q^2/k^2). \tag{6}$$

The second one corresponds to infinitely differentiable regulators that decrease rapidly when $q \gg k$. In practice, for numerical implementations, we use the standard exponential regulator that is, up to field renormalizations,

$$R_k(q) = \alpha \frac{q^2}{e^{q^2/k^2} - 1}. \tag{7}$$

Here the prefactor α has been included in order to study the typical regulator dependence of various results [31].

Before considering our specific analysis of the low temperature phase, let us discuss briefly the approximation scheme employed in the present article, the DE. This corresponds to expanding the Gibbs free energy in the derivatives of the field while keeping any other possible field dependence. For example, at leading order (LPA), it corresponds to taking an arbitrary effective potential and the bare form of the terms including derivatives of the field:

$$\Gamma_k[\phi] = \int d^d x \left\{ \frac{1}{2} \nabla\phi_i(x) \cdot \nabla\phi_i(x) + U_k(\rho) \right\}, \tag{8}$$

where $\rho = \phi_i(x)\phi_i(x)/2$. At next-to-leading order [also called $O(\partial^2)$ order], all possible O(N)-invariant terms involving two derivatives must be included in the *ansatz* of Γ_k:

$$\Gamma_k(\phi) = \int d^d x \left\{ U_k(\rho) + \frac{1}{2} Z_k(\rho) \nabla\phi_i \cdot \nabla\phi_i + \frac{1}{4} Y_k(\rho) \nabla\rho \cdot \nabla\rho \right\} + O(\partial^4). \tag{9}$$

In the particular case of a single scalar field $N = 1$, the third term is redundant and one can in this specific case take $Y = 0$ without loss of generality.

Finally, let us review some difficulties encountered in previous works where the low temperature phase of the O(N) models has been studied with the DE. A more detailed analysis of the corresponding equations is presented in the following sections. The difficulties appear already at LPA level. The flow equation of the derivative of the potential $W_k(\rho) = \partial_\rho U_k(\rho)$ reads

$$\partial_t W_k = -\frac{4v_d}{d} k^{d+2} \left(\frac{3W_k' + 2\rho W_k''}{(k^2 + W_k + 2\rho W_k')^2} + \frac{(N-1)W_k'}{(k^2 + W_k)^2} \right), \tag{10}$$

where $v_d^{-1} = 2^{d+1}\pi^{d/2}\Gamma(d/2)$, $t = \ln(k/\Lambda)$, and the θ regulator, Eq. (6), has been used. At the beginning of the flow, $U_\Lambda(\rho)$ is the bare potential Eq. (5). Accordingly,[2]

$$W_\Lambda(\rho) = r + \frac{u}{3}\rho. \tag{11}$$

[2]For the DE case, we consider $Z_\Lambda(\rho) = 1$ and $Y_\Lambda(\rho) = 0$.

One can control in which phase the system is by computing the position of the minimum of the effective potential $U_{k=0}$ at $k = 0$. At the mean field level, the minimum corresponds to ρ_0, the zero of $W_\Lambda(\rho)$; that is, $-3r/u$ if $r < 0$ or zero if $r \geqslant 0$. Fluctuations tend to lower the value of the average $\langle\varphi\rangle$ of the field and thus of the value of the running minimum $\rho_0(k)$ of U_k when k is decreased. When $T > T_c$, the running minimum hits the origin for a nonvanishing value of k, $\rho_0(k > 0) = 0$, while at T_c it goes to the origin right at $k = 0$. At fixed u, the value of r for which the transition occurs is therefore negative, $\rho_0(k) > 0$ for any $k > 0$ and $\rho_0(k = 0) = 0$. For $T < T_c$, $\rho_0(k)$ remains positive even for $k \to 0$. As a consequence, for the "internal region of the potential," that is, $\rho < \rho_0(k)$, $W_k(\rho) < 0$ for any $k > 0$; see Fig. 1. This is the origin of the difficulties since poles in the denominator of the flow equation (10) can appear because of this negative sign if the regulator is not large enough. For the θ regulator one must require in order to avoid initial singularities that

$$\Lambda^2 + W_\Lambda > 0 \quad \text{and} \quad \Lambda^2 + W_\Lambda + 2\rho W_\Lambda' > 0; \tag{12}$$

that is, $\Lambda^2 + r > 0$ for the particular initial condition (5). These constraints should not be seen as a physical constraint but as a condition on the value of Λ that is appropriate as an initial condition of the flow. By construction the scale Λ must always be much larger than any other physical scale and, accordingly, the previous inequalities must be fulfilled.

When k is lowered, the problem is worse: it has been shown, and will be discussed in detail in the next sections, that when $k \to 0$ in the low temperature phase the flow brings the potential to the regime where $0 < W_k(\rho) + k^2 \ll k^2$. This is numerically even more demanding. Similar observations apply to the LPA equation with other regulators [13].

There is also good news, as has been analyzed before [7,32]. First, in LPA and for some regulators, the singularity works as a barrier in flow equations and consequently the singularity is approached but never reached. Accordingly, the effective potential behaves as $W_k(\rho) \sim -k^2$ in all the internal region. This implies that in those cases, the LPA approximation preserves the convexity of the physical free energy, which becomes flat in the internal region for $k \to 0$, as is shown in the bottom panel of Fig. 1. Second, in the neighborhood of the singularity, the NPRG equation simplifies and analytical solutions can be obtained in that regime [7,32]. In this article following a suggestion made in [13] we exploit analytical solutions in the internal region of the potential in order to construct an efficient algorithm for the broken phase. It must be stressed that in order to do so, it has been necessary to improve considerably previous analytical results. In fact, previous results from [7,32] were only valid at small values of the fields but in order to implement the numerical scheme just mentioned it is necessary to know the analytical form of the solution for larger values of ρ. Such solution is presented here for the LPA approximation and exploited in order to improve qualitatively the quality of the numerical treatment.

Before discussing in detail the analysis of flow equations we want to be precise on the interest of controlling the flow in the "internal" part of the potential because one could say that, finally, what is physically interesting is the region around the minimum of the potential (for zero external field) or the "external" part when one includes an external magnetic field. In some cases, as explained in the introduction, the

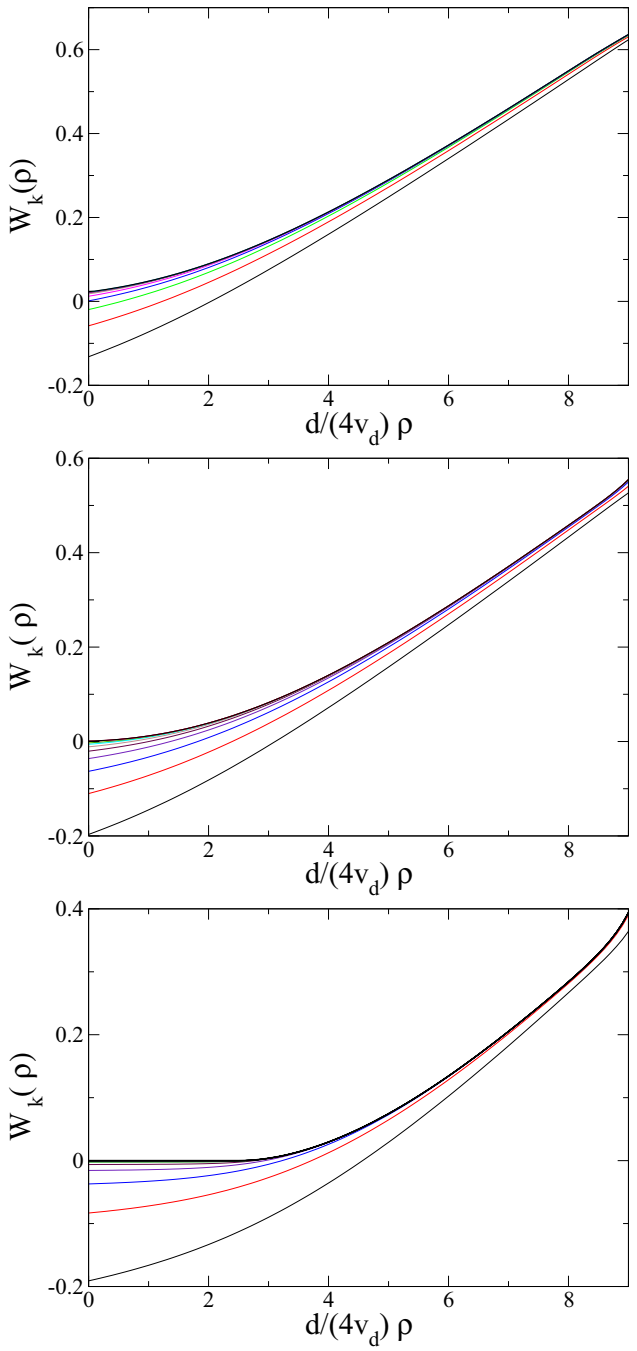

FIG. 1. Top: Typical evolution of the potential to the high temperature phase. Center: Typical evolution near the critical point. Bottom: Typical evolution of the potential in the low temperature phase.

flow stabilized on those parts of the potential before the singularity is reached and one could just stop the flow before the singularity contaminates the physically interesting regions. The problem with this approach is that it is not general because in many other cases the singularity is approached before the region of the potential around the minimum is stabilized. In those (many) cases, one needs to improve the numerical control of the "internal" part of the potential in order to be able to reach small enough values of k. Even more, the notion of "stabilizes" is defined up to a certain precision. If the numerical accuracy around the minimum needs to be improved, sooner or later one will need to address the issue of instabilities in the internal part of the potential.

III. LOCAL POTENTIAL APPROXIMATION

The properties of NPRG equations in the LPA approximation in the broken phase have already been analyzed in the literature both analytically and numerically [7,13,32]. In the present section we briefly review some of these works, generalize them to other cases, and also show some limitations of previous results. After that we exploit the analytical results in order to implement a simple numerical analysis that is significantly more stable than previously considered.[3]

The NPRG equation for the derivative of the effective potential, $W_k = \partial_\rho U_k$, for a generic regulator profile $R_k(q)$ reads [13]

$$\partial_t W_k = -\frac{1}{2}\int \frac{d^d q}{(2\pi)^d}\partial_t R_k(q)\left\{\frac{(N-1)W_k'}{[q^2+R_k(q)+W_k]^2} + \frac{3W_k'+2\rho W_k''}{[q^2+R_k(q)+W_k+2\rho W_k']^2}\right\}. \tag{13}$$

Generalizing the discussion of the introduction, if the flow avoids the presence of singularities, one must have, for all ρ, q, and k,

$$q^2+R_k(q)+W_k > 0, \qquad q^2+R_k(q)+W_k+2\rho W_k' > 0. \tag{14}$$

Now, in the internal region of the potential, one must have, for any k, $W_k < 0$. Accordingly, given that $R_k(q) \sim O(k^2)$, one concludes that, for $q \lesssim k$, $W_k(\rho) = O(k^2)$ (or smaller). On the other hand, in the low temperature phase, the effective potential should have a nontrivial behavior in terms of the physical dimensionful field, or equivalently in terms of ρ.[4] This motivates the use of $w_k(\rho) = W_k(\rho)/k^2$ instead of $W_k(\rho)$. It is convenient to introduce also the dimensionless function $r(y)$ defined by $R_k(q^2) = q^2 r(q^2/k^2)$. With these definitions, the equation for $w_k(\rho)$ reads

$$\partial_t w_k = -2w_k + v_d k^{d-2}\int_0^\infty dy\, y^{d/2+1}\, r'(y) \times\left\{\frac{(N-1)w_k'}{\{y[1+r(y)]+w_k\}^2} + \frac{3w_k'+2\rho w_k''}{\{y[1+r(y)]+w_k+2\rho w_k'\}^2}\right\}. \tag{15}$$

[3] In Ref. [11] an efficient algorithm has been implemented for the LPA approximation of the $N = 1$ case. It is important to observe, however, that it exploits many specificities of this particular case and that it is not trivial to generalize such procedure for other values of N or in more involved approximation schemes.

[4] It must be mentioned that when the system is near a critical regime, a hybrid procedure may be convenient. That is, one can take a rescaling of the field that introduces the standard dimensionless fields at values of k much larger that the physical scales of the problem and becomes just a finite rescaling in the opposite case.

This is in contrast with the usual set of variables used in studies of the critical domain, where w_k is studied as a function of the *dimensionless field* which is, at LPA level, $\tilde{\rho} = \rho/k^{d-2}$.

In the rest of this section we study this equation for various values of N and for various regulators both analytically and numerically. We show that the LPA equation does not avoid the existence of singularities of the flow unless a sufficiently strong regulator is included. In particular, the θ regulator (6) does respect this property. Smooth regulators respect this property also if $1 + R'(q = 0) < 0$ [corresponding to the case $\alpha > 2$ for exponential regulators (7)] [7,13,32]. When this property is not fulfilled, the flow brings the potential to the singularity at $W_k + R(q) = 0$ (typically at $\rho = 0$ and $q = 0$). This case was not fully addressed before in the literature even if such possibility was suggested in [13,32].

A. Large N

We first analyze the large N limit of Eq. (15). This has been done long time ago [32] but we include it here for completeness. Moreover in this case many calculations can be done analytically and this motivates the general behavior of the potential obtained in the general case. The large N limit is taken in the usual way (see, for example, [33]). It is simpler to analyze it for the dimensionful derivative of the potential W_k. The coupling u is of order $1/N$ and U_k and ρ are of order N. Accordingly, W_k is of order 1 and the large N limit of Eq. (13) is

$$\partial_t W_k = -\frac{N}{2} W_k' \int \frac{d^d q}{(2\pi)^d} \frac{\partial_t R_k(q)}{[q^2 + R_k(q) + W_k]^2}. \tag{16}$$

An implicit solution of this differential equation can be obtained by considering the inverse function $\rho = F_k(W)$ [32]. It satisfies $F_k'(W) = 1/W_k'(\rho)$ and $\partial_t F_k(W) = -F_k'(W)\partial_t W_k(\rho)$. Accordingly

$$\partial_t F_k(W) = \frac{N}{2} \int \frac{d^d q}{(2\pi)^d} \frac{\partial_t R_k(q)}{[q^2 + R_k(q) + W]^2}. \tag{17}$$

In this equation W must be seen as an independent variable and consequently (17) can be integrated:

$$F_k(W) - F_\Lambda(W) = -\frac{N}{2} \int \frac{d^d q}{(2\pi)^d} \left\{ \frac{1}{q^2 + R_k(q) + W} - \frac{1}{q^2 + R_\Lambda(q) + W} \right\}. \tag{18}$$

Given an initial condition for the potential, one can invert it in order to obtain $F_\Lambda(W)$. For example, for a Hamiltonian of the form (5), one obtains, by inverting the relation between $W_k(\rho)$ and ρ,

$$F_\Lambda(W) = \frac{3}{u}(W - r). \tag{19}$$

If Λ is much larger than any other physical scale, one can absorb for $d < 4$ the dependence on Λ in a renormalization of the parameter r, obtaining an implicit equation for $W_k(\rho)$:

$$\rho - \frac{3}{u}[W_k(\rho) - \tilde{r}] = -v_d N k^{d-2} \int_0^\infty dy\, y^{d/2-1} \times \left(\frac{1}{y[1 + r(y)] + W_k(\rho)/k^2} - \frac{1}{y} \right), \tag{20}$$

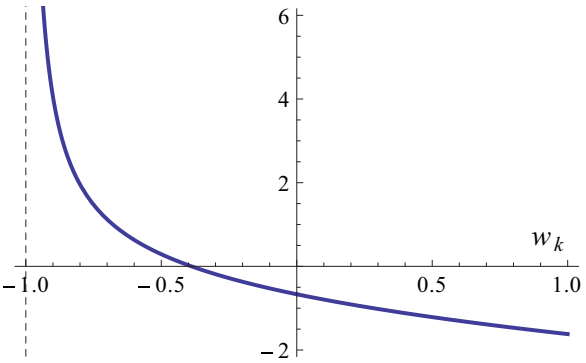

FIG. 2. Right hand side of Eq. (22) as function of w_k.

where

$$\tilde{r} = r + \frac{Nu}{6} \int \frac{d^d q}{(2\pi)^d} \left\{ \frac{1}{q^2} - \frac{1}{q^2 + R_\Lambda} \right\} \tag{21}$$

is the renormalized mass parameter. We can see here that the minimum of the potential goes to zero when $k \to 0$ only if $\tilde{r} = 0$. One deduces that $\tilde{r} \propto (T - T_c)$ near the phase transition. We use this equation now in order to study the behavior for various regulators and, in particular, analyze how the convexity is approached in the low temperature phase and if and when the singularity can be reached at a nonzero value of k. As expected, there is only a broken phase for $d > 2$ because for $d \leqslant 2$ the integral in (21) is infrared divergent.

Let us consider now how this equation behaves for specific regulators. Let us consider first the θ regulator (6), which allows integrals to be done analytically at integer dimensions. For example, for $d = 3$,

$$\left[\frac{3}{u}(w_k k^2 - \tilde{r}) - \rho\right]/(2v_3 N k) = \begin{cases} -1 + \frac{1}{3+3w_k} - \sqrt{w_k}\arctan(\sqrt{w_k}) & \text{if } w_k \geqslant 0, \\ -1 + \frac{1}{3+3w_k} + \sqrt{|w_k|}\operatorname{arctanh}(\sqrt{|w_k|}) & \text{if } w_k < 0. \end{cases} \tag{22}$$

Here we used as before the notation $w_k(\rho) = W_k(\rho)/k^2$. In Fig. 2, the right hand side of Eq. (22) is plotted as a function of w_k; we can see that it diverges when $w_k(\rho) \to -1$. In Fig. 3 the numerical solution of the implicit Eq. (22) is shown for typical parameters in the low temperature phase. One observes that the singularity, $w_k(\rho) = -1$, is approached by the solution in the internal region of the potential. Moreover, in Fig. 4, it can be seen that the singularity is approached but is not crossed. This is very similar to the results obtained in [13] except that it was not known that the θ regulator leads exactly to (22). In fact, the approach of the singularity can be discussed analytically. First of all, the right hand side of Eq. (22) is a monotonic decreasing function. Accordingly it is not difficult to convince oneself that a unique solution exists for any ρ and k. This means that the singularity is never reached. Second, if the singularity is not crossed and a low temperature phase exists, there are values of ρ with $w_k < 0$ for all $k > 0$. There are then only two possibilities. The first one corresponds either to $w_k \to 0^-$ or to a negative constant larger than -1 in the internal region. However, if this were true, the right hand side of Eq. (22) would tend to a constant and the left hand side would tend to

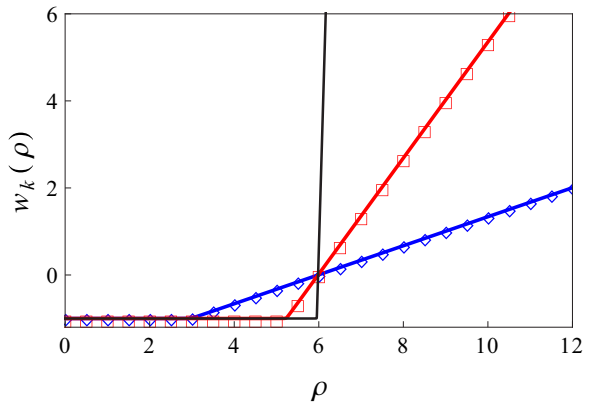

FIG. 3. Solution of Eq. (22) for $w_k(\rho)$ as a function of ρ for various values of $k = 10^{-2}\Lambda$ (blue diamonds), $k = 10^{-3}\Lambda$ (red squares), and $10^{-4}\Lambda$ (black plain line).

infinity when $k \to 0$ giving a contradiction. Correspondingly, the only remaining possibility is that $w_k(\rho)$ tends to -1 in all the internal region of the effective potential. Consequently, one can make an expansion of Eq. (22) in $\delta w_k(\rho) = w_k(\rho) + 1$. At leading order one obtains

$$\delta w_k(\rho) = \frac{2v_3 N}{3} \frac{k}{-3\tilde{r}/u - \rho}, \tag{23}$$

which, as observed before, leads to $\delta w_k(\rho)$ going to zero when $k \to 0$ for all $\rho < -3\tilde{r}/u$.

One can repeat this calculation for arbitrary integer dimension, but it is convenient to generalize it to an arbitrary d by performing the expansion on $\delta w_k(\rho)$ directly at the level of flow equations. This allows the generalization of this procedure to arbitrary values of N. Before doing that, let us show the corresponding result for large values of N. If one expands at leading order on $\delta w_k(\rho)$ the flow equation (10) (taken at large N) one arrives at

$$\left(\frac{1}{\delta w_k(\rho)}\right)' \sim -\frac{dk^{2-d}}{2v_d N} \tag{24}$$

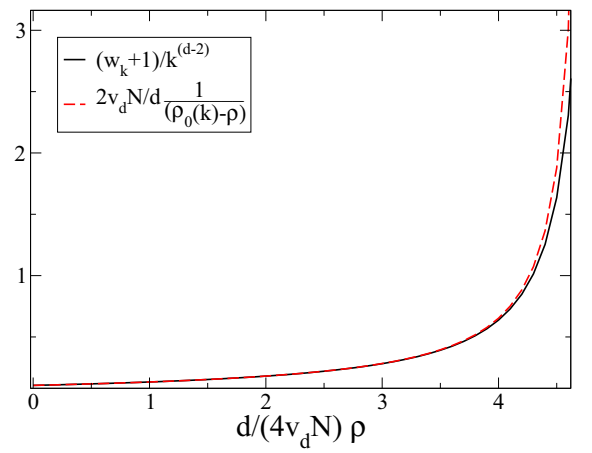

FIG. 4. Comparison of numerical (black plain line) and semianalytical (red dashed) solutions for $w_k + 1$ at large N as a function of ρ for the θ regulator ($d = 3$) for $k = 0.002$.

whose solution is

$$\delta w_k(\rho) = \frac{2v_d N k^{d-2}}{d} \frac{1}{\hat{\rho}_0(k) - \rho}. \tag{25}$$

Here $\hat{\rho}_0(k)$ is an integration constant that cannot be fixed without referring to the full (analytical or numerical) solution from the microscopic scale Λ to the infrared limit ($k \to 0$). In the particular large N case, this constant can be fixed analytically as in (23). In the $k \to 0$ limit, moreover, it must be identified with $\rho_0(k = 0)$ because, as discussed before, in the entire internal zone of the potential, the approximation just analyzed becomes correct when $k \to 0$. From the solution of this equation we observe that the limit of validity of this approximation is precisely $\rho < \rho_0(k = 0)$ when $k \to 0$. Another consequence of this general solution is that there is no broken phase in LPA for $d \leqslant 2$ (as expected from the Mermin-Wagner theorem): For $d \leqslant 2$, the "correction" does not tend to zero, and the associated solution does not exist. Following the previous discussion, the only possibility, in the absence of singularities, is that at a given $k_0 > 0$, the minimum of the effective potential reaches $\rho = 0$ and remains there after.

The results from the numerical solution of (10) (taken at large N) coincides with the previous results. One can solve the equation with a standard finite differences explicit Euler procedure (with typical parameters $\Delta\rho = 0.034$ and $\Delta t = -10^{-5}$). In Fig. 4 the corresponding results are shown. Both solutions agree with good precision for values of ρ for which $w_k(\rho) < 0$. However, the singularity is approached and eventually the numerical code brings the potential to the wrong side of the singularity and the flow blows up. This is a purely numerical problem. In fact, by improving the parameters of the numerical code one can push the flow to smaller values of k. However, given that the singularity is approached rapidly it becomes impossible to go to really small values of k by simply taking smaller grids and larger volumes in ρ. To solve this problem, we will present below an improved numerical algorithm that solves this difficulty.

The large N limit of the LPA equation (16) and its solution (20) have been partially analyzed previously for smooth regulators such as the exponential one [7,13]. In fact, there are essentially two typical cases (see Fig. 5): case (i) the inverse propagator $y[1 + r(y)] + W_k(\rho)/k^2$ has its minimum at a nonzero value of y (let us call it y_0), and case (ii) the inverse

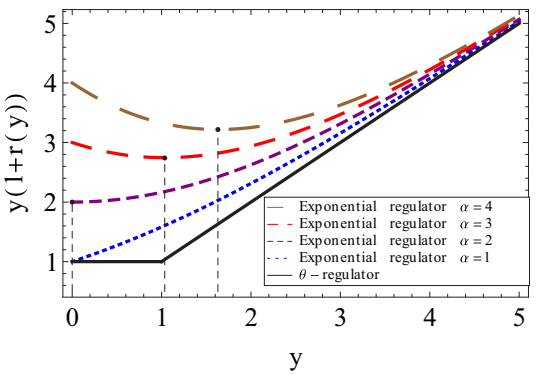

FIG. 5. $y[1 + r(y)]$ for different regulators. The vertical dashed lines show the minimum of $y[1 + r(y)]$, y_0, for each case.

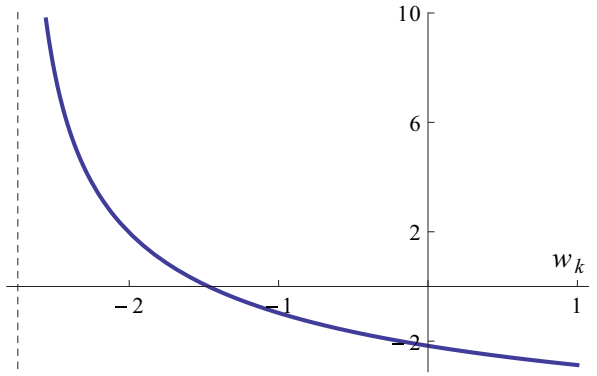

FIG. 6. Right hand side of Eq. (20) for the exponential regulator and $\alpha = 3$ ($d = 3$). The dotted line points out the position of the singularity $-y_0[1 + r(y_0)]$.

propagator has its minimum at $y = 0$ with the derivative of the inverse propagator with respect to y being positive at $y = 0$. For the exponential regulator (7) the case (i) corresponds to the case $\alpha > 2$ (i.e., for a strong enough regulator) and the case (ii) corresponds to the case $\alpha < 2$. There is a third possible case that corresponds to a minimum of the inverse propagator at $y = 0$, the derivative of which is zero. That is a very peculiar possibility that should be analyzed case-by-case.

Let us discuss first case (i). It has been shown that in this case, the behavior of the flow in the low temperature phase is qualitatively similar to the one analyzed for the θ regulator [7,13]: the singularity works as a barrier that is approached but never crossed and accordingly the convexity of the effective potential is ensured by the LPA equation. The exponent characterizing the approach to the singularity does not depend on the specific form of the regulator profile but is different from the particular case of the θ regulator. The right hand side of Eq. (20) diverges when $W_k(\rho)/k^2$ approaches $-y_0[1 + r(y_0)]$. It is not hard to convince oneself that this singularity comes from the region of integration $y \approx y_0$. This can be seen in Fig. 6 where the right hand side of Eq. (20) is represented in the case $\alpha = 3$.

Accordingly, one can obtain the equivalent of the integral when the singularity is approached by substituting in the numerator of the integral y with y_0 and by expanding the denominator at leading nontrivial order [at order $(y - y_0)^2$]. Equation (20) near the singularity becomes

$$\rho - \frac{3}{u}[W_k(\rho) - \tilde{r}] = -v_d N k^{d-2} \int_{-\infty}^{\infty} \frac{dy\, y_0^{d/2-1}}{\delta w_k + C(y - y_0)^2} = -v_d N k^{d-2} \frac{\pi\, y_0^{d/2-1}}{\sqrt{C\,\delta w_k}}, \tag{26}$$

where the notations $\delta w_k = y_0[1 + r(y_0)] + W_k(\rho)/k^2$ and $C = r'(y_0) + y_0 r''(y_0)/2$ have been introduced. In this equation, the integration domain has been enlarged from $-\infty$ because this integration domain is regular in the limit $\delta w_k \to 0$. It is important to observe that the $(\delta w_k)^{-1/2}$ behavior does not depend on the precise shape of the regulator as long as it has a regular behavior around y_0, the minimum at nonzero value of y, and as long as C, the second derivative of the inverse propagator at y_0, is nonzero. This second hypothesis

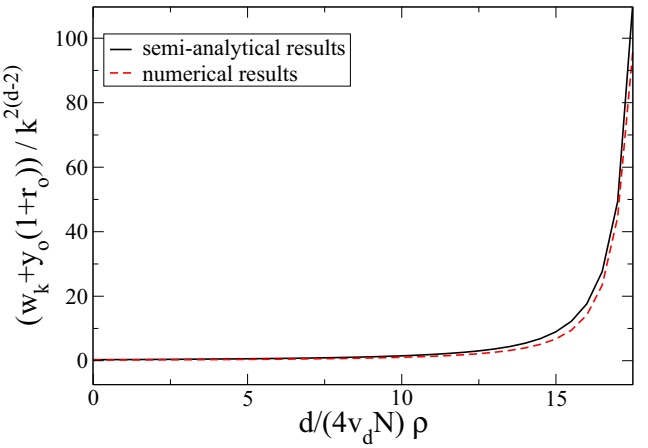

FIG. 7. Comparison of numerical (black plain line) and semi-analytical (red dashed) solutions at large N for $w_k + y_0[1 + r(y_0)]$ as a function of ρ for the exponential regulator ($d = 3$). Curves for $k = 0.08$.

is not fulfilled by the θ regulator and this is why the right hand side of Eq. (20) has a different behavior. In fact, when $n - 1$ derivatives of the inverse propagator with respect to y are zero at y_0, the behavior of the right hand side of Eq. (18) is as $(\delta w_k)^{-1+1/n}$, the θ regulator corresponding to the limit $n \to \infty$.

Equation (26) can now be inverted by observing that, for the same reasons invoked for the θ regulator, the singularity is approached but never reached. Accordingly when $k \to 0$, one can expand Eq. (26) on δw_k. At leading order, one obtains

$$\delta w_k(\rho) = \frac{1}{C}\left(\frac{v_d N k^{d-2} \pi\, y_0^{d/2-1}}{\rho_0 - \rho}\right)^2 \tag{27}$$

with $\rho_0 = -3\tilde{r}/u$. As done for the θ regulator, one can also obtain a similar expression by integrating directly the flow equation (16). One obtains the same expression, except that ρ_0 is replaced by an arbitrary function of k, $\hat{\rho}_0(k)$, that comes as an integration constant (independently of ρ). As before, in the limit $k \to 0$, $\hat{\rho}_0(k)$ can be interpreted as the position of the minimum of the effective potential $\rho_0(k = 0)$.

We display in Fig. 7 a numerical solution of the LPA equation in the large N limit (16) that has been obtained, as before, using finite differences and an explicit Euler method with typical parameters $\Delta\rho = 0.034$ and $\Delta t = -10^{-5}$. It must be stressed that to observe numerically the proper behavior of the solution in the internal region of the potential is much more numerically demanding than, for example, to study the critical behavior of these models (in that case one can typically obtain stable results with $\Delta\rho/k^{d-2} = 0.1$ and $\Delta t = -2 \times 10^{-3}$). The only difference from the θ regulator is that the integrals over momenta must be done numerically. We employ for this purpose Simpson's rule with a regular grid in momenta with 80 steps of a dimensionless momentum step of 0.1. The solution agrees with the analytical behavior just presented. However, as with the θ regulator, at a certain value of k, the singularity is crossed due to numerical lack of precision and consequently the flow collapses. As with the θ regulator, we present below a more elaborated method in order to avoid such collapse.

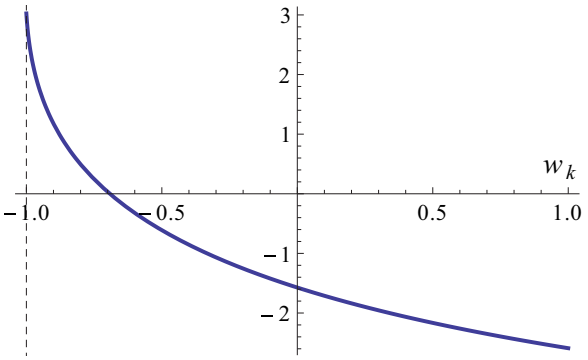

FIG. 8. Right hand side of Eq. (20) for the exponential regulator and $\alpha = 1$ ($d = 3$). The dotted line point out the position of the singularity $-\tilde{R} = -\lim_{y\to 0} y[1 + r(y)]$.

Let us now consider the case (ii) (corresponding to $\alpha < 2$ in the particular case of the exponential regulator). In this case, the singularity does not work any more as a barrier and the integral remains bounded when the singularity is approached. The singularity in that case shows up first at $y = 0$, and corresponds to the point where $w_k(\rho)$ approaches $-\tilde{R} \equiv -\lim_{y\to 0} y[1 + r(y)]$. The integral is not differentiable at $w_k(\rho) = -\tilde{R}$ but remains continuous at this point. In the particular case of the exponential regulator (7), $\tilde{R} = \alpha$. As mentioned before, the flow blows up at a finite scale k_0 because U_k hits the singularity at $k = k_0$. This singularity, which occurs at finite k, is also observed when numerically integrating the flow equation. However, this is not very conclusive because when $\alpha > 2$, the singularity that should not be reached in principle is actually reached in practice because of numerical inaccuracies. In order to be fully convinced that the singularity is hit, one can exploit the implicit large N solution (20) and observe that there is a solution for $w_k = -\tilde{R}$ when ρ and k are small enough. In order to see that, one can observe that the right hand side of Eq. (20) is bounded from above as a function of w_k. As an example, in Fig. 8, the case $\alpha = 1$ is represented. One sees that the right hand side presents a singularity but that it is finite, not diverging. As a consequence, nothing forbids the large N implicit solution (20) to reach the singularity at $k > 0$.

Having discussed the standard numerical solution of the equation, the implicit analytical solution, and the explicit analytical solution near the singularity, we present now an improved numerical solution that exploits the obtained analytical behavior in the two cases discussed above where the singularity is avoided: the θ regulator and the smooth regulator in case (i). The idea is simple and has been already suggested (but not implemented) in [13]. One can employ a standard numerical procedure at typical points in a grid, but in a region where the solution is close enough to the singularity [and where the analytical solutions (25) or (27) are therefore justified], one replaces the result of the flow equation by the analytical expressions (25) or (27), depending on the chosen regulator. For a given smooth regulator, the constant y_0 can be calculated (by looking at the minimum of $y[1 + r(y)]$). For values of ρ at which w_k is above a chosen threshold, one implements a standard numerical solution (finite differences plus explicit Euler). The value of the integration

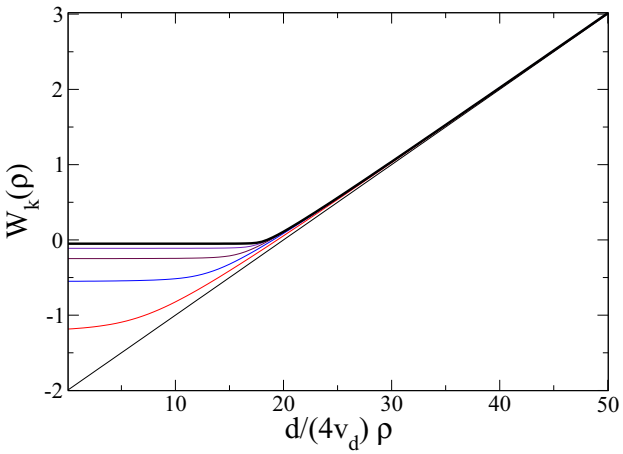

FIG. 9. Derivative of the potential at large N and $d = 3$ as a function of ρ for various values of k (lower curves are for larger values of k).

constant $\hat{\rho}_0(k)$ is taken in order to require the continuity between the analytical solution below the threshold and the purely numerical one above it. It must be stressed that this algorithm requires the knowledge of the solution in the full internal region and not only around $\rho = 0$ as was obtained in [7,32]. For actual numerical implementations with the θ regulator we took the value for the threshold at $w_k = -0.98$. In the case of the exponential regulator, we chose $\alpha = 3$ (for which $y_0 \simeq 1.035658$) and we chose the threshold value $w_k = -2.74$. This numerical procedure is completely stable. The flow can be continued down to $k/\Lambda \sim 1.5 \times 10^{-8}$ without encountering any difficulty. From the result of w_k one can reconstruct the dimensionful potential which, as expected, is convex. The corresponding result is shown in Fig. 9.

The large N limit is not particularly exciting because the flow equation can be essentially solved analytically and because physically interesting models correspond to lower values of N. We merely use it to test various ideas about the approach to convexity. In the following we exploit such ideas to more realistic values of N, beginning with the $N = 1$ and finally generalizing to other values of N.

B. Finite N

We analyze now the the finite N case, where no (even implicit) analytical solution is known. As done for large N we consider the corresponding equations (10) and (13) both analytically and numerically, first with the θ regulator and then for a generic smooth regulator (the corresponding numerical implementation is performed for the exponential one).

Consider first the LPA flow equation with the θ regulator for $N = 1$:

$$\partial_t w_k = -2w_k - \frac{4v_d}{d} k^{d-2} \frac{3w_k' + 2\rho w_k''}{(1 + w_k + 2\rho w_k')^2}. \qquad (28)$$

Again, let us admit (as clearly seen in the numerical solution of the equation in $d = 3$) that the LPA equation displays a low temperature phase in which there is a minimum of the potential $\rho_0(k)$ with $w_k(\rho_0(k)) = W_k(\rho_0(k))/k^2 = 0$ for any $k > 0$ and with $\rho_0(k = 0) > 0$. Repeating a similar analysis to the one

performed for large N, one concludes that the flow approaches the singularity where $1 + w_k(\rho) + 2\rho w_k'(\rho) = 0$. In that case there are, again, two possibilities: either the singularity is never reached or it is crossed.

It is difficult to give a general analytical proof for finite N that the singularity is not crossed at any finite value of k, but the numerical solution of the equations gives clear indications in this direction for the θ regulator. Under this hypothesis, one concludes that when k is small enough the flow approaches a regime when $1 + w_k(\rho) + 2\rho w_k'(\rho)$ is small in all the internal region of the potential but positive. Moreover, in the absence of singularities for $k > 0$, $w_k(\rho)$ is a regular function of ρ. The solution of the equation

$$1 + w_k(\rho) + 2\rho w_k'(\rho) \approx 0 \tag{29}$$

is

$$w_k(\rho) \approx -1 + A_k/\sqrt{\rho}, \tag{30}$$

where A_k is an arbitrary function of k. One observes that typical solutions of (29) have a singularity at $\rho = 0$. However, by hypothesis the singularity is not reached and consequently solutions of full flow equations are regular for all values of ρ (including $\rho = 0$) when $k > 0$. One must then restrict oneself to the only solution among (30) that is regular corresponding to $A_k = 0$ for any k. One concludes that $1 + w_k(\rho) + 2\rho w_k'(\rho) \approx 0$ is equivalent to $1 + w_k(\rho) \approx 0$ in the entire internal region of the potential. This is the same behavior as for large N but for a slightly subtler reason. Moreover, as when N is large, one can analyze the approach to this regime by expanding Eq. (28) in $\delta w_k(\rho) = w_k(\rho) + 1$:

$$\frac{4v_d}{d} k^{d-2} \frac{3\delta w_k' + 2\rho \delta w_k''}{(\delta w_k + 2\rho \delta w_k')^2} = 2 + O(\delta w_k). \tag{31}$$

Neglecting the term $O(\delta w_k)$ on the right hand side, one can solve Eq. (31). The solutions that are regular at $\rho \sim 0$ are of the form

$$\delta w_k(\rho) = \frac{v_d}{d} \frac{k^{d-2}}{\sqrt{\rho_0(k)\rho}} \ln\left(\frac{\sqrt{\rho_0(k)} + \sqrt{\rho}}{\sqrt{\rho_0(k)} - \sqrt{\rho}}\right), \tag{32}$$

where $\rho_0(k)$ is an arbitrary function depending on the initial conditions of the flow. Given that this solution is only valid for small values of k, a possible k dependence of ρ_0 can be neglected. The value of $\rho_0(k)$ is in the $k \to 0$ limit the position of the minimum of the effective potential. It is interesting to note that the expression (32) shows quite explicitly a well-known artifact of the LPA approximation: there is no low temperature phase, even for $N = 1$, within this approximation in $d = 2$. One observes that the supposedly "small correction" does not tend to zero for $d = 2$ breaking the self-consistency of the analysis. Moreover, explicit numerical solutions do not find broken phases for that dimension. We will see below that this difficulty is corrected by the $O(\partial^2)$ order of the DE.

For generic values of N, the LPA equation with the θ regulator is

$$\partial_t w_k = -2w_k - \frac{4v_d}{d} k^{d-2} \left(\frac{3w_k' + 2\rho w_k''}{(1 + w_k + 2\rho w_k')^2} + \frac{(N-1)w_k'}{(1 + w_k)^2}\right). \tag{33}$$

The two convexity conditions to be fulfilled are those of large N and of $N = 1$. As explained before, and admitting that both singularities are not crossed at finite k, both of them imply that when k is small, $\delta w_k(\rho) = w_k(\rho) + 1 \ll 1$. As in previous cases, one can expand Eq. (33) in δw_k yielding the differential equation

$$\rho_0(k) - \rho = \frac{2v_d}{d} k^{d-2} \left(\frac{1}{\delta w_k + 2\rho \delta w_k'} + \frac{N-1}{\delta w_k}\right), \tag{34}$$

where $\rho_0(k)$ is an arbitrary function depending on initial conditions. As before, $\rho_0(k)$ can be interpreted when $k \to 0$ as the position of the minimum for the potential, and one can neglect its k dependence. Equation (34) cannot be solved analytically except for the previously considered cases ($N = 1$ and large N).[5] Since it is a differential equation one could expect that for any ρ_0 it has an infinite number of solutions corresponding to different choices of $\delta w_k(\rho = 0)$. However, as before, one must require that it be well behaved in all the domain of validity of the approximation, and in particular for $\rho = 0$. This fixes the value of $\delta w_k(\rho = 0)$ in terms of ρ_0:

$$\delta w_k(\rho = 0) = \frac{2v_d}{d} k^{d-2} \frac{N}{\rho_0(k)}, \tag{35}$$

yielding a single regular solution in the domain of validity of the equation. Equation (34) can be solved numerically easily. It is convenient to define

$$u = \frac{\rho}{\rho_0(k)}, \qquad f(u) = \frac{\delta w_k(\rho)}{\delta w_k(\rho = 0)}, \tag{36}$$

which yields the following equation for $f(u)$:

$$1 - u = \frac{1}{N}\left(\frac{1}{f(u) + 2uf'(u)} + \frac{N-1}{f(u)}\right) \tag{37}$$

with the initial condition $f(u = 0) = 1$. The expression of $\delta w_k(\rho)$ can be reconstructed from that of $f(u)$ obtained at a given N and for an arbitrary $\rho_0(k)$:

$$\delta w_k(\rho) = \frac{2v_d}{d} k^{d-2} \frac{N}{\rho_0(k)} f(\rho/\rho_0(k)). \tag{38}$$

The form of $f(u)$ for various values of N obtained by numerically solving Eq. (37) is shown in Fig. 10. It must be stressed that the *correction* to $\delta w_k \approx 0$ depends on N. However, for any N one generically approaches the regime where $\delta w_k \approx 0$ but the corresponding function $f(u)$ depends on N for generic values of ρ in the internal region. Our analysis is consistent with the previous one because in the $\rho \to 0$ limit the correction matches its large N limit as is expected from [7,32].

We also solve numerically the LPA equation with the θ regulator for various values of N with the same procedure presented before for large N. First, we solve it directly using

[5] In fact, at $N = 0$ the case can be handled analytically also. In that case, a δw_k independent of ρ is the solution of (34). If one ask for the continuity of the solution when $N \to 0$, the solution is [see (35)] completely fixed.

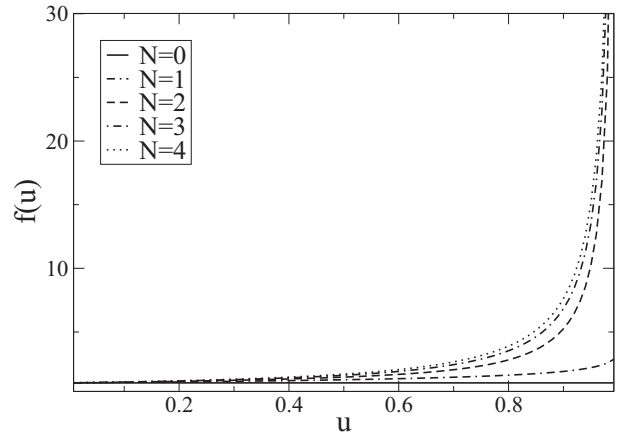

FIG. 10. $f(u)$ as a function of u for various values of N.

finite differences for the derivatives and an explicit Euler algorithm for the evolution in t. Typically the parameters used are $\Delta\tilde{\rho} = 0.1$ and $\Delta t = -10^{-5}$. As can be seen in Fig. 11, in all cases (including $N = 0$), a low temperature phase is found for $d > 2$ and the numerical solution indicates that the function $w_k(\rho)$ approaches (without crossing) -1 in all

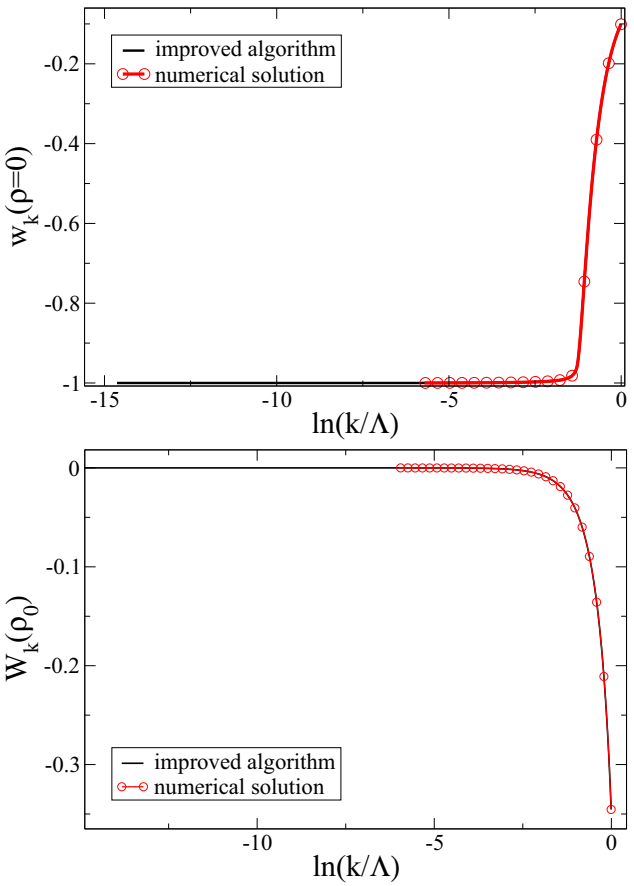

FIG. 11. Top: $w_k(\rho = 0)$ as a function of $t = \ln(k/\Lambda)$. Bottom: $W_k(\rho_0)$ where $\rho_0 = \lim_{k\to 0} \rho_0(k)$ as a function of $t = \ln(k/\Lambda)$. In both cases, the curves are for $N = 4$ and $d = 3$. Comparison between the direct numerical solution (red circles) and the improved algorithm (black plain line) in both cases with the θ regulator.

the internal region of the potential. However, as for large N, when the solution is too close to the singularity it may happen that discretization errors lead to an artificial crossing of the singularity.

It is interesting to note that the numerical implementation of the LPA equation for $N = 1$ turns out to be much more difficult than for $N > 1$. The reason for this result, at first sight surprising, is twofold. First, as explained before, for $N > 1$ the convexity condition $w_k(\rho) > -1$ is imposed directly by the term of the LPA Eq. (13) proportional to $N - 1$. The other term of the right hand side of the equation (the only one present when $N = 1$) imposes the weaker constraint $w_k(\rho) + 2\rho w_k'(\rho) > -1$ that eventually leads to the same consequence $[w_k(\rho) > -1]$ but in a much more indirect way (see above). Numerically this effect seems to be harder to control. The second and more important reason is that, for $N = 1$, the dimensionful physical effective potential $U_{k=0}$ has a discontinuity in its second derivative at the minimum of the potential (see, for example, [34]). This is simply related to the fact that for $N = 1$ the susceptibility [given by the inverse of $2\rho_0 w_k'(\rho_0)$] is finite both in the high and low temperature phase (only diverging asymptotically when the critical temperature is approached). This implies that $w_k'(\rho_0) > 0$ whereas $w_k'(\rho < \rho_0) \to 0$ for $k \to 0$ due to convexity of the potential and so $w_k'(\rho)$ develops a discontinuity when $k \to 0$. On the contrary, the second derivative of the physical effective potential is continuous for $N > 1$, even at the minimum $[w_k'(\rho \leqslant \rho_0) \to 0$ when $k \to 0]$. This expresses the fact that both the longitudinal and transverse susceptibilities of the O(N) models with continuous symmetries ($N > 1$) are infinite for any temperature below the critical one because of Goldstone mode fluctuations. In practice, the effective potential for $k > 0$ remains much more regular around the minimum for $N > 1$ diminishing the sources of instabilities.

In order to improve the stability of the numerical solution, we employed the same procedure presented above for large N: we fixed a threshold $w^{\text{threshold}} = -0.95$, solved numerically the flow equation (13) when $w_k(\rho)$ is above $w^{\text{threshold}}$, and imposed the quasianalytical form given by Eq. (38) for $w < w^{\text{threshold}}$. The implementation of this procedure proves to be essentially stable at arbitrary values of t for all $N > 1$. We must stress the first point where the singularity related to the numerical violation of the convexity is $\rho = 0$. In this concern, this is the more demanding point and for this reason we analyzed in detail the behavior of the function $w_k(\rho = 0)$. A typical example of such solution is shown on the top part of Fig. 11. It shows that the improved algorithm is much more stable than the direct integration of the equation. However for most values of t, the flow comes for $\rho = 0$ from the semianalytical solution. In order to see the solution for values of ρ where the semianalytical solution is not implemented for any t, it is shown in the bottom part of Fig. 11 the value of $W_k(\rho_0)$ where $\rho_0 = \lim_{k\to 0} \rho_0(k)$. As expected, $W_k(\rho_0) \to 0$ for $k \to 0$. More interestingly, one observes that the numerical solution can be extended for values of k that are many orders of magnitude smaller than without the algorithmic improvement.

As before, the numerical solution of Eq. (13) for $N = 1$ is much more demanding. In fact, the procedure explained above does not work for $N = 1$ as efficiently as in the $N > 1$

case, although (31) is again a good approximation in all the internal region of the potential. It turns out that the mismatch between the second derivatives of the potential at the matching point corresponding to $w^{\text{threshold}}$ is large enough to generate numerical instabilities. We must insist on the existence of a *second kind* of singularity around the minimum of the potential at large $|t|$. The reason, as stated before, is that the physical effective potential is not analytical in this point. For $N > 1$ our improved algorithm becomes finally unstable because the numerical solution becomes sensitive to this late-time singularity [which, as explained before, is a discontinuity in the first derivative of $W_{k=0}(\rho)$ for $N = 1$ and in the second derivative for $N > 1$]. Only after the singularity for $\rho = 0$ is under control, this second derivative can be studied with precision.

We analyzed the equation also for typical smooth regulators. Again, there are two different cases, depending on the position of the minimum of $y[1 + r(y)]$. As for large N, when the minimum takes place at a $y = y_0 > 0$, integrals on the right hand side of the LPA equation can be approximated as in (26). Accordingly the singularities play the role of a barrier that cannot be crossed and one arrives at a scenario very similar to the one of the θ regulator: the singularity is approached but never crossed. In this case the behavior of the analytical solution when $k \to 0$ is

$$\delta w_k \sim k^{2(d-2)} f(\rho). \tag{39}$$

For for $N = 1$ the function $f(\rho)$ can be found analytically,

$$f(\rho) = \frac{1}{C^2}\left[\frac{1}{\rho_0^{3/2}\sqrt{\rho}} \ln\left(\frac{\sqrt{\rho}+\sqrt{\rho_0}}{\sqrt{\rho_0}-\sqrt{\rho}}\right) + \frac{2}{\rho_0(\rho_0-\rho)}\right],$$

and for $N > 1$ it can be obtained by solving the differential equation:

$$f + 2\rho f' = \frac{1}{\left[\frac{C}{2}(\rho_0 - \rho) - \frac{N-1}{\sqrt{f}}\right]^2}.$$

In both cases the constant C is related to the minimum as

$$C = \frac{y_0[1 + r(y_0)]}{v_d y_0^{d/2} r(y_0)\pi}\sqrt{r'(y_0) + y_0 r''(y_0)/2}.$$

Following the same procedure we can go further in the solution of the flow equation as shown on the top of Fig. 12. The improvement is not as good as for the θ regulator. This is due to the fact that the approach to the singularity is faster [for the θ regulator the exponent in k is $d - 2$, see Eq. (35), and for the smooth regulator the exponent is $2(d - 2)$, see Eq. (39)] than for the θ-regulator case. Therefore, the solution becomes flat faster and the matching point of the improved algorithm approaches the minimum very quickly. As a consequence, the physical nonanalyticity around the minimum is approached also faster. Let us emphasize that the singularity related to the numerical violation of the convexity is solved by the improved algorithm in both cases as well. The origin of the differences is that the *physical* singularity around the minimum destabilizes the flow for the smooth regulator faster. For completeness we include also on bottom of Fig. 12 the evolution of $W_k(\rho)$, as was done for the θ regulator in order to observe the flow in a value of ρ where the semianalytical solution is never directly implemented.

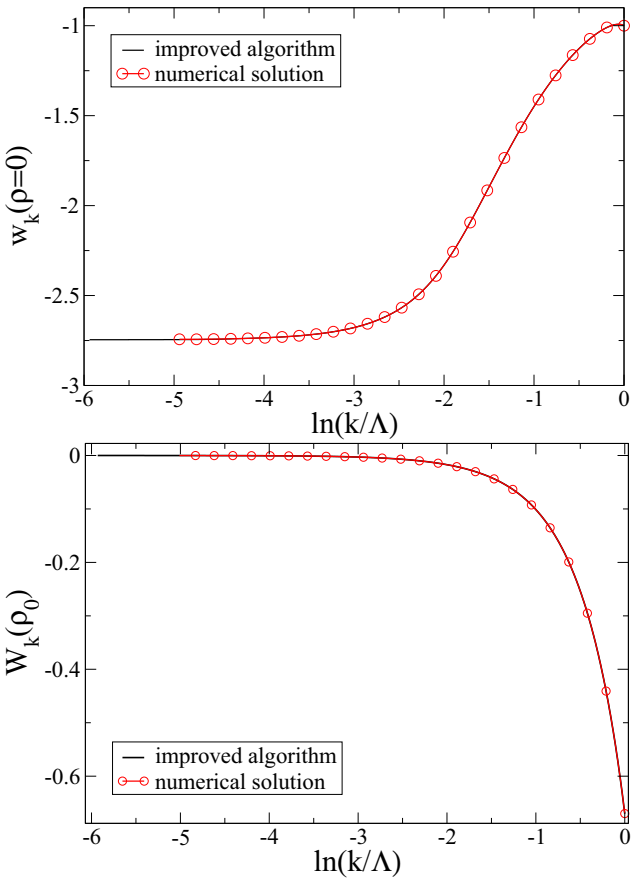

FIG. 12. Top: $w_k(\rho = 0)$ as a function of $t = \ln(k/\Lambda)$. Bottom: $W_k(\rho_0)$ where $\rho_0 = \lim_{k\to 0} \rho_0(k)$ as a function of $t = \ln(k/\Lambda)$. In both cases, the curves are for $N = 4$ and $d = 3$. Comparison between the direct numerical solution (red circles) and the improved algorithm (black plain line) in both cases with the exponential regulator for $\alpha = 3$.

Having discussed the treatment of the LPA equation in the various cases and showing a numerical algorithm that is much more stable than the standard one for all $N > 1$, we consider now the next-to-leading order of the derivative expansion.

IV. DERIVATIVE EXPANSION AT ORDER $O(\partial^2)$

In this section, we generalize the previous numerical studies on the approach to a convex free energy at the LPA level to second order in the derivative expansion. This approximation corresponds to an expansion to second order of the NPRG equation in powers of the external momenta; see Eq. (9). We derived the corresponding NPRG equations and we verified the equivalence with [35].[6] We limit ourselves to a direct numerical analysis leaving for the future an analytical study analogous to the one performed for the LPA. This analysis should again improve the numerical integration of the flow equations but the number of cases to be studied brings it clearly beyond the scope of the present article. One aspect

[6]In the numerical algorithm we use $w_k(\rho) = W_k/(Z_k k^2)$, $Z_k(\rho)/Z_k$, and $Y_k(\rho)/Z_k$ as variables when solving the flow.

that cannot be addressed at the LPA level is the broken phase for $N = 1$ in $d = 2$ since the running of the field renormalization factor is neglected which artificially destroys the broken phase. On the contrary, at order $O(\partial^2)$ of the DE, a phase transition is found at finite temperature for $N = 1$ in $d = 2$ [35]. For $N > 2$, no phase transition is found with this approximation in agreement with the Mermin-Wagner theorem and for $N = 2$, the Kosterlitz-Thouless phase transition is correctly described [35–37].[7]

An important difference between the order $O(\partial^2)$ of the DE and the LPA is that it is convenient to introduce a prefactor in the regulator function $R_k(q)$ that evolves with k (as usually done in the study of the critical regime). This prefactor has many purposes in the critical regime.[8] In the present case let us consider the inverse propagator (for $N = 1$ for example):

$$G_k^{-1}(q) = q^2 Z_k(\rho) + W_k(\rho) + 2\rho W_k'(\rho) + \hat{R}_k(q). \quad (40)$$

For $\hat{R}_k(q)$ to regulate efficiently and for all values of k the small wave number modes, it is necessary that it is at least of the same order as $q^2 Z_k(\rho)$ up to $q \sim k$. As usual, we use regulators of the form

$$\hat{R}_k(q) = Z_k R_k(q) \quad (41)$$

where $R_k(q)$ are the regulator profiles used at the LPA level, see Eqs. (6) and (7), and Z_k is fixed as $Z_k(\rho)$ at a particular value of ρ. The difficulty is that $Z_k(\rho)$ depends strongly on ρ and, not surprisingly, the behavior of this function for ρ larger or smaller than the minimum of the potential is very different in the low temperature phase when $k \to 0$. We analyze two possible choices: ρ larger or smaller than ρ_0, the minimum of the potential when $k \to 0$. As we will see, the appropriate choice for this point depends on the value of N. On one hand, when $N > 1$, we observe that the flow is more stable if Z_k is taken as the value of $Z_k(\rho)$ for a $\rho > \rho_0$, in some cases in a very significant way. For this reason, for those values of N, all results presented below correspond to this choice of ρ (more precisely, $\rho = 2\rho_0$). On the other hand, for $N = 1$, one must fix the value of Z_k for a ρ in the "internal" part of the potential, as explained below. If this is not done, the flow of the potential hits the singularity as with the LPA for a regulator not strong enough. As for the choice of the regulator profile, the main advantage of the θ regulator (6) is lost at the second order of the DE because the integrals cannot be performed any more analytically. We therefore use the exponential regulator (7) in what follows and we choose a prefactor α larger than 2 to avoid singularities in the flow; see Sec. III.

The large N case is not particularly useful for the second order of the derivative expansion, because in that limit, the LPA equation for the potential becomes exact. We consider then, first, the single scalar case, generalizing those results to the O(N) case after. An analysis of such theories has been done a few years ago at the second order of the derivative expansion in [12] but for $d = 4$. Here we consider dimensions $d < 4$ that are generically much richer for scalar theories. Moreover, an interesting but very weak logarithmic divergence of the function $Z(\rho) + \rho Y(\rho)$ was observed in [12]. In $d < 4$, we observe clearer and stronger effects because the corresponding divergence is a power law, as will be discussed below.

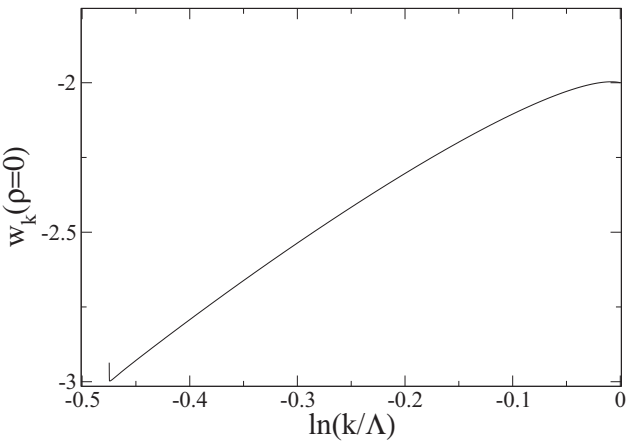

FIG. 13. $w_k(\rho = 0)$ as a function of $t = \ln(k/\Lambda)$ for $N = 1$ and $d = 3$ using the exponential regulator (7) with $\alpha = 3$. Normalization fixed at $\rho = 2\rho_0$.

A. Single scalar case

As said before, in the $N = 1$ case, one can simply take $Y_k = 0$. As seen in Fig. 13, when the renormalization factor Z_k in the regulator profile is chosen for values of ρ in the "external" part of the effective potential, the flow collapses after a certain renormalization group "time." When $\rho_{\text{ren}} > \rho_0$, the flow blows at a finite RG time because there is no barrier preventing the singularity to be reached. The reasons are the following: (i) In the external part, the function $Z_k(\rho)$ rapidly stabilizes and accordingly the function Z_k becomes a constant below a finite value of k. (ii) The flow of $Z_k(\rho)$ in the "internal" part continues to grow without bound. (iii) For all $k > 0$ in the internal part, the potential is not convex. Accordingly, the regulator becomes negligible in the internal part of the potential and the flattening of the internal part is not strong enough to avoid the singularity (as is the case for the LPA with an exponential regulator with $\alpha < 2$). For $N = 1$ we therefore choose Z_k as the value of $Z_k(\rho)$ at $\rho = 0$.

With this choice, we observe as in the LPA case that the effective potential runs in the low temperature phase to a convex potential that is flat in the "internal" part but that finally collapses when, due to numerical lack of precision, the singularity of the flow equation is crossed. We observe systematically that if the discretization parameters of the program are improved, the instability appears at larger renormalization group "times" (indicating that this phenomenon is a numerical artifact), but, in practice, they are finally reached.

A typical run of the effective potential is shown in Fig. 14 for $d = 3$. We observe a potential approaching the convexity. In Fig. 15 the flow of the function $Z_k(\rho)$ is presented (also for

[7]The cases with $N < 1$ in any dimension and, in particular, the physically interesting case $N = 0$ require an independent analysis that goes beyond the present article. In that case, the sign of the term in the potential equation proportional to $N - 1$ changes and, consequently, a different analysis is required.

[8]For example, this prefactor makes the fixed point condition of NPRG equations identical to the Ward identity of scale transformations in the presence of an infrared regulator; see [38].

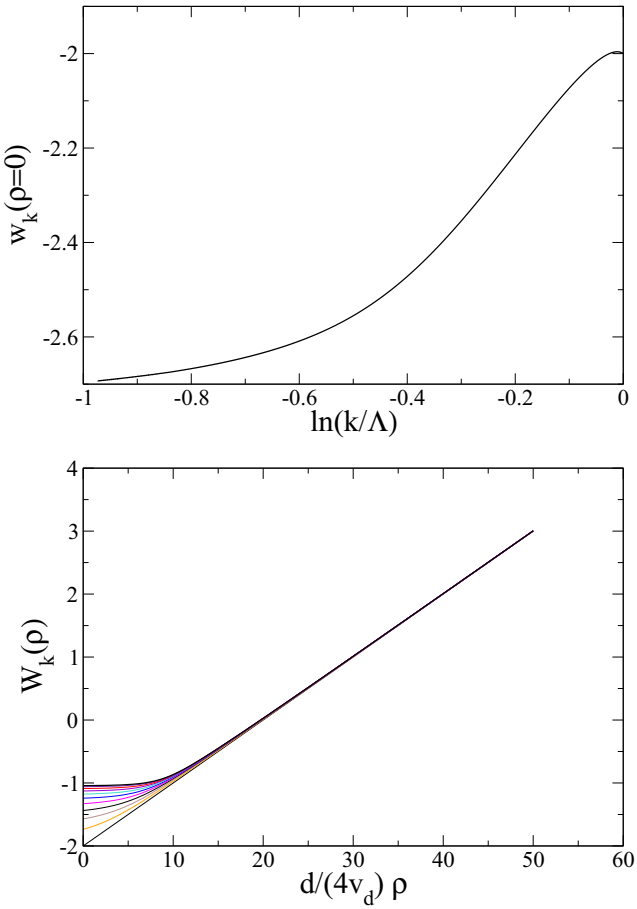

FIG. 14. Top: $w_k(\rho = 0)$ as a function of $t = \ln(k/\Lambda)$. Bottom: $W_k(\rho)$ as a function of ρ for various values of t ranging from 0 to -1. In both figures, $N = 1$ and $d = 3$ using the exponential regulator (7) with $\alpha = 3$ and normalization fixed at $\rho = 0$.

$d = 3$). As expected, in the "external" part of the potential the function $Z_k(\rho)$ stabilizes when $k \to 0$, as can be seen clearly in the inset of Fig. 15. However, one observes that the function $Z_k(\rho)$ seems to diverge when $k \to 0$ for values of ρ in the

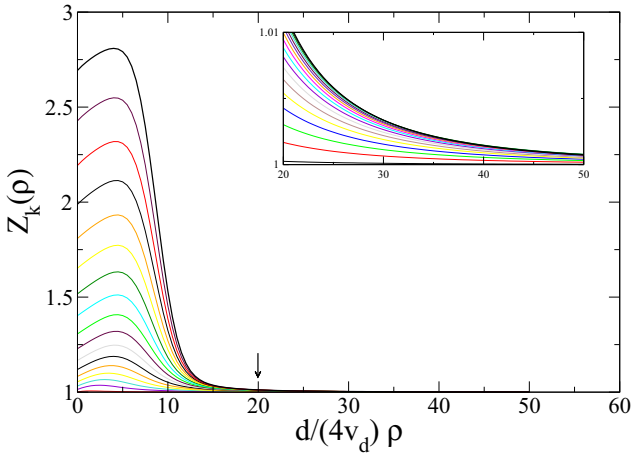

FIG. 15. $Z_k(\rho)$ for $N = 1$ and $d = 3$ using the exponential regulator (7) with $\alpha = 3$. Normalization fixed at $\rho = 0$. The arrow shows the last position of the minimum reached by the simulation.

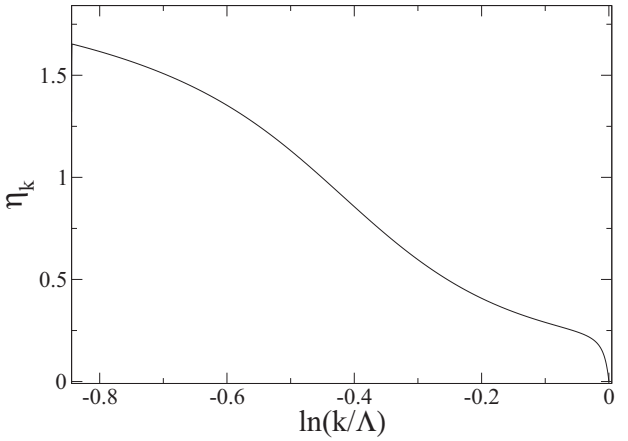

FIG. 16. η_k for $N = 1$ and $d = 3$ using the exponential regulator (7) with $\alpha = 3$. Normalization fixed at $\rho = 0$. Observe that, given that $Z_k(\rho = 0)$ and $Z_k(\rho = 2\rho_0)$ are different, the position of the singularity is different from the LPA order.

"internal" part of the potential. In order to study how this divergence takes place, we plot in Fig. 16 the quantity $\eta_k = -\partial_t \ln Z_k$ that shows the exponent of the divergence of $Z_k(\rho = 0)$ as a function of t. We observe that the exponent seems to stabilize at values $\sim$1.5 but at that value of t the singularity is hit and the flow breaks down. It is important to stress that the running exponent η_k is *not* the physical exponent that must approach zero for $N = 1$ in the broken phase. The present η_k exponent is extracted from the behavior of $Z_k(\rho = 0)$ and the physical exponent must be extracted from the behavior of $Z_k(\rho)$ at the minimum. As can be seen in the inset of Fig. 15, the function stabilizes in the external part of the potential. Accordingly the physical exponent goes to zero, as it must.

As we just explained, for the purpose of having a numerical algorithm that avoids the singularities related to the convexity one must take a regulator with a prefactor Z_k that evolves with $Z_k(\rho = 0)$ but as shown in Fig. 17 the behavior of $Z_k(\rho)$ is completely different in both points. In Fig. 17 the renormalized function

$$\hat{Z}_k(\rho) = \frac{Z_k(\rho)}{Z_k(\rho = 0)} \tag{42}$$

is plotted. It seems to approach a finite limit for values of ρ corresponding to the "internal" part of the potential and, as expected, to tend to zero in the "external" part [given the fact that the function $Z_k(\rho)$ seems to go to a finite limit in that regime]. As a conclusion, the second order of the DE seems to respect the convexity property and the singularity present in the flow equation for the potential does not seem to be hit. However, a standard numerical implementation finally breaks down (as in the LPA) because of the unavoidable lack of precision.

As said before, contrarily to what happens at the LPA level, the second order of the DE clearly shows for the single scalar case a low temperature phase not only in $d = 3$ but also in $d = 2$. This is shown in Figs. 18, 19, and 20. As explained before, this is one of the most important ingredients absent at the LPA level and one of the main reasons to go beyond. The

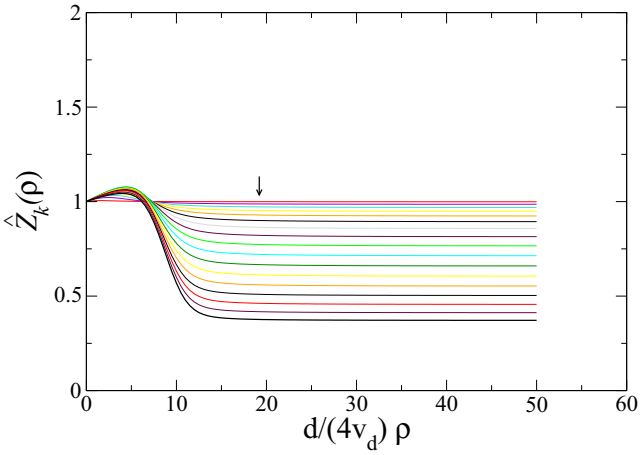

FIG. 17. $\hat{Z}_k(\rho)$ as function of ρ for various values of t for $N = 1$ and $d = 3$ using the exponential regulator (7) with $\alpha = 3$. Normalization fixed at $\rho = 0$. The arrow shows the last position of the minimum reached by the simulation.

results for $d = 2$ seem to be qualitatively similar to those of $d = 3$ for $N = 1$.

B. Generic O(N) model

In this section we extend the analysis of the second order of the derivative expansion in the low temperature phase for $N > 1$.

In this case, in contrast to the $N = 1$ one, choosing Z_k at values larger than ρ_0 turns out to give a more stable flow than the one obtained if Z_k is fixed at ρ smaller than ρ_0. When Z_k is fixed at values larger than ρ_0 the flow does not explode until large values of $|t|$. Figure 21 shows that, as for LPA, a convex potential is approached along the flow. As before, we need to choose a value of α larger than 2 to avoid hitting the singularity. We employed an Euler algorithm of the same kind as the one employed in the LPA (without the improvement in the internal part of the potential). Even if convexity is clearly visible we are not able to reach very large values of $|t|$, because of the same numerical instabilities discussed before. In any case, as for the LPA approximation, the flow for $N > 1$ is much more stable than for the $N = 1$. It is very plausible that a hybrid algorithm that exploits the exact behavior of NPRG equations in the internal region would, as for the LPA case, allow one to make the flow even more stable.

It is interesting to discuss also the results for the flows of the functions $Z_k(\rho)$ and $Y_k(\rho)$. In fact, we prefer to present the results in terms of the transverse renormalization function $Z_k(\rho)$ and the longitudinal one, $Z_k(\rho) + \rho Y_k(\rho)$, as shown in Figs. 22 and 23. As one can observe, the function $Z_k(\rho)$ seems to reach a limit when $k \to 0$. In contrast, the longitudinal renormalization factor $Z_k(\rho) + \rho Y_k(\rho)$ seems to grow without bound around the minimum of the potential. This is similar to what is observed in $d = 4$ in [12]. However, in the $d = 3$ the effect is much stronger. In fact, it is expected to growth proportional to $1/k$. This is due to the fact that the longitudinal propagator behaves as $1/|q|$ in $d = 3$ and around the minimum it also behaves as the inverse of $q^2[Z_k(\rho_0) + \rho_0 Y_k(\rho_0)]$. We checked this behavior in Fig. 24.

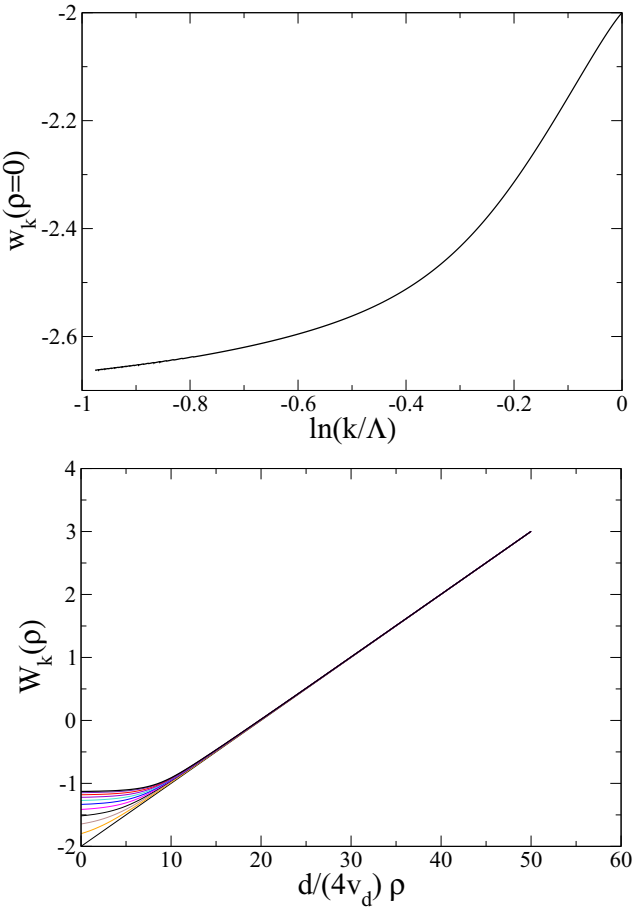

FIG. 18. Top: $w_k(\rho = 0)$ as a function of $t = \ln(k/\Lambda)$. Bottom: $W_k(\rho)$ as a function of ρ for different values of t. In both figures, for $N = 1$ and $d = 2$ using the exponential regulator (7) with $\alpha = 3$ and normalization fixed at $\rho = 0$.

In what concerns the behavior of these functions in the "external" region of the potential, it seems to stabilize faster. This can be seen in the running of the anomalous dimension (fixed via the value of Z_k at $2\rho_0$) as can be seen in Fig. 22. One

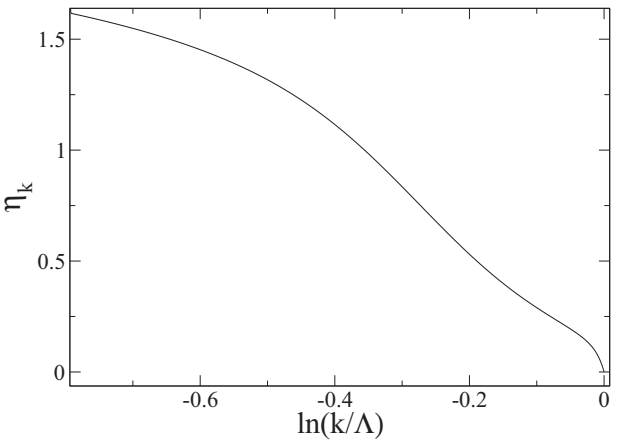

FIG. 19. η_k for $N = 1$ and $d = 2$ using the exponential regulator (7) with $\alpha = 3$. Normalization fixed at $\rho = 0$.

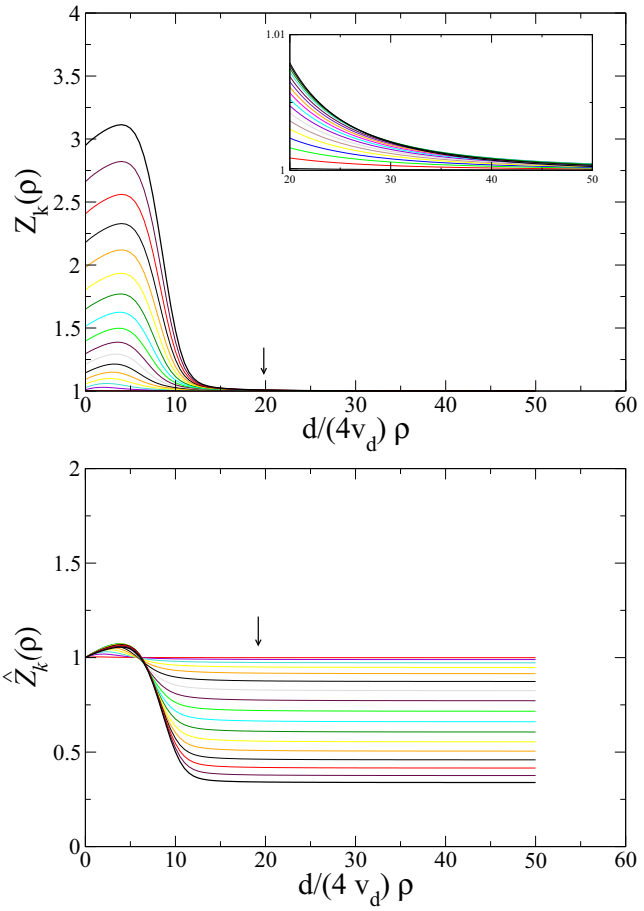

FIG. 20. Top: $Z_k(\rho)$ as a function of ρ. Bottom: $\hat{Z}_k(\rho)$ as function of ρ. In both cases, for various values of t for $N = 1$ and $d = 2$ using the exponential regulator (7) with $\alpha = 3$. Normalization fixed at $\rho = 0$. The arrows show the last position of the minimum reached by the simulation.

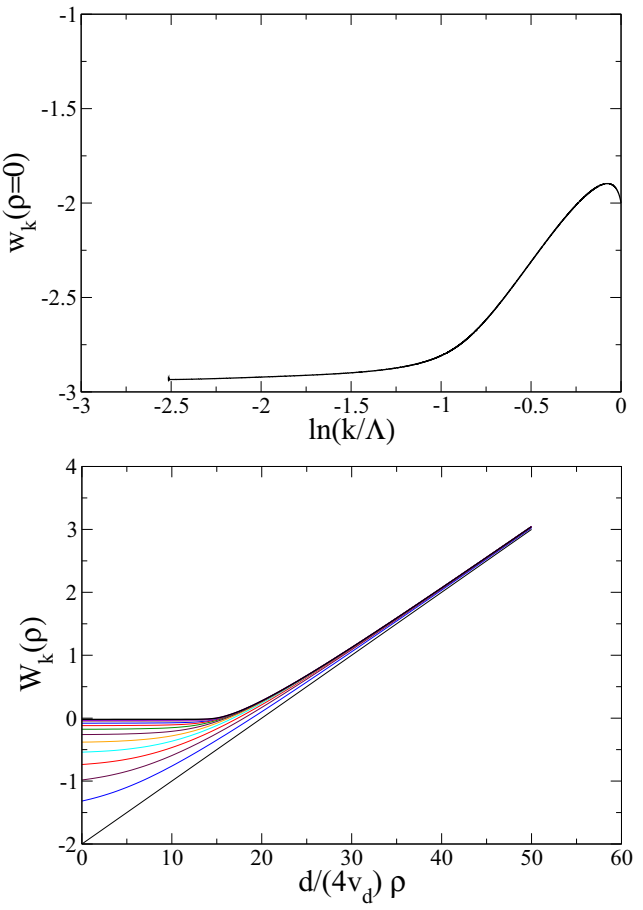

FIG. 21. Top: $w_k(\rho = 0)$ as a function of $t = \ln(k/\Lambda)$. Bottom: $W_k(\rho)$ as a function of ρ for various values of t. In both figures, for $N = 4$ and $d = 3$ using the exponential regulator (7) with $\alpha = 3$ and normalization fixed at $\rho = 2\rho_0$.

observes that η_k goes to zero as expected in the low temperature phase.

We have thus managed to study the low temperature phase of O(N) models in the second order of the DE and shown that if an appropriate regulator and renormalization condition is used, one can show clearly that the property of convexity of the effective potential is respected. The flow finally becomes unstable for numerical reasons. When $N > 1$ the flow is much more stable than in the single scalar case $N = 1$.

V. CONCLUSIONS

In the present article we analyze the NPRG equations both at the leading order (LPA) of the derivative expansion and at next-to-leading order (order ∂^2) in the low temperature phase. These simple approximations performed at the level of NPRG equations are able, in contrast with most perturbative schemes, to preserve the convexity of the free energy. Our study shows that this is only true for certain regulators. In particular, the most used regulators (the θ regulator and the exponential regulator) are able to respect the convexity of the free energy. However, in the case of the exponential regulator, it is necessary to choose a large enough prefactor. If this is not done, a singularity of the flow is hit. Contrarily to common wisdom, quite large prefactors for the exponential regulator are needed in order to have nonsingular flows. In particular, a standard exponential regulator with $\alpha = 1$ gives a singular flow in the low temperature. This may be surprising because this

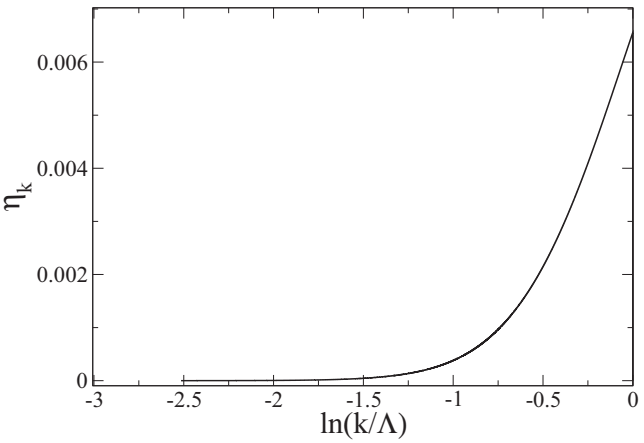

FIG. 22. η_k as a function of t for $N = 4$ and $d = 3$ using the exponential regulator (7) with $\alpha = 3$. Normalization fixed at $\rho = 2\rho_0$.

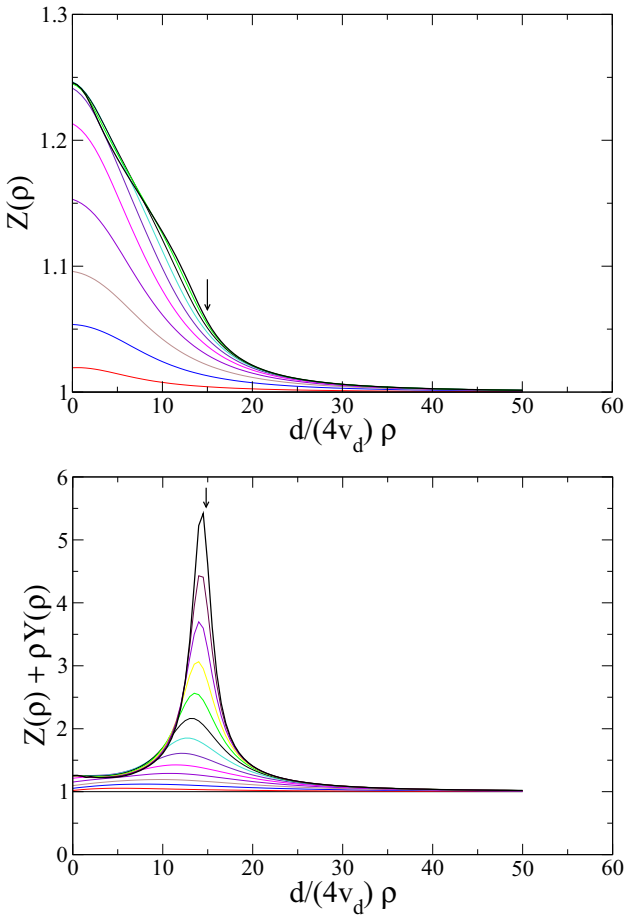

FIG. 23. Top: $Z_k(\rho)$ as a function of ρ. Bottom: $Z_k(\rho) + \rho Y_k(\rho)$ as function of ρ, for various values of t for $N = 4$ and $d = 3$ using the exponential regulator (7) with $\alpha = 3$. Normalization fixed at $\rho = 2\rho_0$. The arrows show the last position of the minimum reached by the simulation.

regulator works perfectly well in the critical regime showing that the low temperature phase is even more difficult to handle that the critical point.

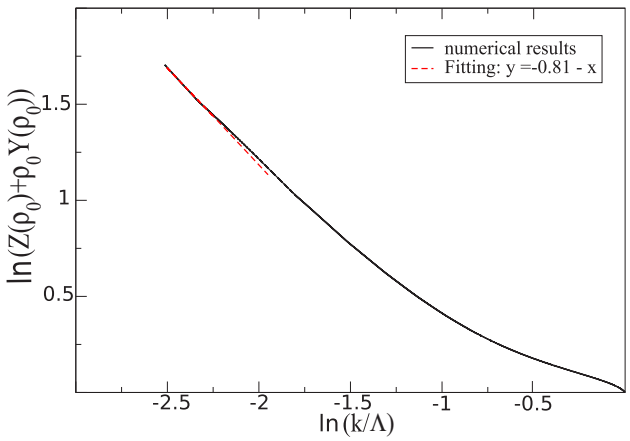

FIG. 24. $\ln[Z_k(\rho_0) + \rho_0 Y_k(\rho_0)]$ as a function of $\ln(k/\Lambda)$.

Even if an appropriate regulator is chosen, there is a practical difficulty: the flow approaches a singularity without crossing it. As a consequence, even if the singularity is never hit, the flow becomes numerically unstable for low enough values of k. In order to deal with this problem many algorithms have been proposed in the literature. We implement at the LPA level a very simple algorithm that exploits the exact behavior of the flow in the "internal" part of the potential and that makes the flow stable for essentially arbitrary values of k when $N > 1$. The $N = 1$ case turns out to be much more challenging for various reasons discussed along the article. The most important one comes from the fact that the physical longitudinal susceptibility is a continuous function of the external field for $N > 1$ but has a discontinuity for $N = 1$ when $k \to 0$. This makes this case much harder to treat. We obtain for $N > 1$ and with a very simple algorithm a flow that is qualitatively more stable than what was obtained before.

On top of this analysis, we studied the behavior of the flow in the low temperature phase at order ∂^2 of the derivative expansion. We observe that in order to approach a convex free energy it is necessary to normalize the field in a different way in the case $N = 1$ and in the case $N > 1$. On one hand, in order to avoid reaching the singularity of the flow for $N = 1$ it is necessary to normalize the field in the "internal" region of the potential. On the other hand, in the $N > 1$ case it is necessary to normalize the field in the "external" part of the potential. Once these choices are made and an appropriate regulator is chosen, the flow approaches a convex free energy. Of course, in practice, the flow becomes numerically unstable when k is very small and the numerical flow hits the singularity.[9]

For the future, we are planning to implement the same kind of algorithm that we presented in the LPA case at second order of the derivative expansion $O(\partial^2)$. We are planning also to make the same kind of analysis in more elaborated approximations such as the one proposed in [22–24]. We would like also to try to implement an improved algorithm in these kinds of approximations.

These improved approximations and algorithms in the low temperature phase of O(N) models could be useful in the analysis of a large variety of physical problems that we are planning to address, such as the formation of bound states or the calculation of the phase diagram and the equation of state for realistic microscopic models. In particular, as mentioned in the introduction, bound states in the broken phase near criticality [25] have been recently analyzed with the NPRG and we plan to exploit the methods developed in the present article in order to extend those results to more involved cases.

ACKNOWLEDGMENTS

The authors acknowledge financial support from the ECOS-Sud France-Uruguay program U11E01, and from the PEDECIBA. We thank also B. Delamotte, N. Dupuis, M. Tissier, and F. Benitez for useful discussions.

[9]The two-dimensional XY case [36] has been studied in Refs. [35,37]. In that case, the singularity seems always reached [37]. It must be stressed that this low temperature phase is very peculiar.

[1] C. Wetterich, Phys. Lett. B **301**, 90 (1993).
[2] U. Ellwanger, Z. Phys. C **58**, 619 (1993).
[3] N. Tetradis and C. Wetterich, Nucl. Phys. B **422**, 541 (1994).
[4] T. R. Morris, Int. J. Mod. Phys. A **09**, 2411 (1994).
[5] T. R. Morris, Phys. Lett. B **329**, 241 (1994).
[6] A. Ringwald and C. Wetterich, Nucl. Phys. B **334**, 506 (1990).
[7] N. Tetradis and C. Wetterich, Nucl. Phys. B **383**, 197 (1992).
[8] A. Horikoshi, K.-I. Aoki, M.-A. Taniguchi, and H. Terao, arXiv:hep-th/9812050.
[9] J. Alexandre, V. Branchina, and J. Polonyi, Phys. Lett. B **445**, 351 (1999).
[10] A. S. Kapoyannis and N. Tetradis, Phys. Lett. A **276**, 225 (2000).
[11] J.-M. Caillol, Nucl. Phys. B **855**, 854 (2012).
[12] D. Zappalà, Phys. Rev. D **86**, 125003 (2012).
[13] J. Berges, N. Tetradis, and C. Wetterich, Phys. Rep. **363**, 223 (2002).
[14] B. Delamotte, Lect. Notes Phys. **852**, 49 (2012).
[15] L. Canet, H. Chaté, and B. Delamotte, J. Phys. A **44**, 495001 (2011).
[16] M. Tissier and G. Tarjus, Phys. Rev. Lett. **107**, 041601 (2011).
[17] G. R. Golner, Phys. Rev. B **33**, 7863 (1986).
[18] L. Canet, B. Delamotte, D. Mouhanna, and J. Vidal, Phys. Rev. B **68**, 064421 (2003).
[19] I. Balog, L. Canet, H. Chaté, and B. Delamotte (unpublished).
[20] V. Pangon, S. Nagy, J. Polonyi, and K. Sailer, Int. J. Mod. Phys. A **26**, 1327 (2011).
[21] V. Pangon, Int. J. Mod. Phys. A **227**, 1250014 (2012).
[22] J.-P. Blaizot, R. Méndez Galain, and N. Wschebor, Phys. Lett. B **632**, 571 (2006).
[23] F. Benitez, J.-P. Blaizot, H. Chaté, B. Delamotte, R. Méndez-Galain, and N. Wschebor, Phys. Rev. E **80**, 030103 (2009).
[24] F. Benitez, J.-P. Blaizot, H. Chaté, B. Delamotte, R. Mendez-Galain, and N. Wschebor, Phys. Rev. E **85**, 026707 (2012).
[25] F. Rose, F. Benitez, F. Léonard and B. Delamotte, Phys. Rev. D **93**, 125018 (2016).
[26] B. Delamotte (private communication).
[27] U. Ellwanger, Z. Phys. C **62**, 503 (1994).
[28] T. Machado and N. Dupuis, Phys. Rev. E **82**, 041128 (2010).
[29] A. Rancon and N. Dupuis, Phys. Rev. B **84**, 174513 (2011).
[30] D. Litim, Phys. Lett. B **486**, 92 (2000); Phys. Rev. D **64**, 105007 (2001); Nucl. Phys. B **631**, 128 (2002); Int. J. Mod. Phys. A **16**, 2081 (2001).
[31] L. Canet, B. Delamotte, D. Mouhanna, and J. Vidal, Phys. Rev. D **67**, 065004 (2003).
[32] N. Tetradis and D. F. Litim, Nucl. Phys. B **464**, 492 (1996).
[33] M. D'Attanasio and T. R. Morris, Phys. Lett. B **409**, 363 (1997).
[34] N. Dupuis, Phys. Rev. E **83**, 031120 (2011).
[35] G. Von Gersdorff and C. Wetterich, Phys. Rev. B **64**, 054513 (2001).
[36] J. M. Kosterlitz and D. J. Thouless, J. Phys. C **6**, 1181 (1973).
[37] P. Jakubczyk, N. Dupuis, and B. Delamotte, Phys. Rev. E **90**, 062105 (2014).
[38] B. Delamotte, M. Tissier, and N. Wschebor, Phys. Rev. E **93**, 012144 (2016).